Proceedings of the International Gas Turbine Congress 2003 Tokyo
November 2-7, 2003

Micro- or Small- Gas Turbines

Terrence W. Simon and Nan Jiang

Department of Mechanical Engineering
Heat Transfer Laboratory
University of Minnesota

ABSTRACT

Recently, increased attention has been paid to small gas turbine units. Microturbines with fuel cells and microturbines with heaters in a Combined Heat and Power (CHP) arrangement are showing great promise for supplying distributed electric and shaft power and process or space heat. Small jet engines are becoming increasingly popular for small piloted and non-piloted aircraft.

In developing the microturbine for power generation, considerable attention has been paid to improving the recuperator, which had not seen such intensive research and development activity since the years of automobile gas turbine development. Also, the small size of the microturbine has led to a preference for radial turbomachinery, including radial inflow turbines. Smaller turbomachinery and other components have led to greater interest in ceramic components and ceramic coatings. Renewed interest in radial flow turbomachinery revealed a need to better understand radial-flow component fluid mechanics such as the effects of streamline curvature on boundary layer flows. Finally, small sizes have raised attention to low Reynolds number effects, such as transition and flow separation, particularly in the development of small axial-flow turbines for use in aircraft propulsion.

In this report, we review recent developments documented in the literature for these areas of interest to small gas turbine engines and comment on contributions from our research lab.

INTRODUCTION

INTEREST IN DISTRIBUTED ELECTRIC POWER GENERATION

A major change in US energy policy began in 1978 with the Public Utilities Regulatory Policies Act (PURPA). This gave birth to an independent power industry by ending regional monopolies over the generation of electricity. This led to many changes, including a growth in microturbine sales; 300 in 1999 to 5,000 in 2001. Deregulation led to considerable confusion, however, about how to proceed. After the disastrous summer of 2001 in California, many states chose to proceed with great caution. Presently, generation of power can be national (even international), though the control is often still local. Previously, generation, transmission and distribution were "bundled" into one customer bill. Now they are "unbundled," where generation and transmission may be by competitors, though distribution is usually with the "incumbent suppliers." This led to restrictions on availability of shared transmission facilities and more interest in distributed power generation. Also, experience with interrupted power led to a new market, "high grade" power capable of supporting the "digital world." Digital servers cannot afford occasional interruptions and are willing to pay a premium for reliable, uninterrupted power. Also, opportunities for bartering pollution credits with "green energy" production have emerged where businesses have the opportunity to purchase "certificates" to offset the environmental effects of added facilities. This has opened opportunities for microturbines or other distributed sources to burn "green fuels," such as municipal and agricultural wastes. Recently, concern arose over disruption of power by terrorist acts, directing more attention to distributed power to reduce the effect of a single mishap.

In the last two years, the US suffered a downturn of its economy resulting in reduced demand for energy and relaxation in national energy planning. Coincidentally, much of the enthusiasm for growth in distributed power has waned. On August 14, 2003, a portion of North America suffered a massive, though short-lived, blackout. This served as a reminder that federal attention must be paid to power generation and distribution. When the economy rebounds, the demand of the past will reemerge with, perhaps, heightened demand for distributed power generation. Given a worldwide economic recovery, as anticipated, the shortages and concerns may be more acute than in the past. In anticipation, the engineering community must continue with development of systems available for efficient distributed power generation. In this next phase, we anticipate that microturbines will have an increased share of the power system.

INTEREST IN SMALL ENGINES AND LOW-REYNOLDS NUMBER FLOWS IN AIRCRAFT PROPULSION

In recent years, the commercial air transportation market has moved to more, direct routes and a mild reduction of the use of airline hubs. This has driven the commercial airline business to manufacture more, small aircraft. Since propeller-driven small aircraft are becoming less acceptable to the modern short trip passengers, these aircraft are increasingly using small ducted fan gas turbine engines. Also, the military is becoming more reliant on small Unpiloted Aviation Vehicle (UAV) aircraft, for which the jet engine is becoming an increasingly attractive propulsion option. Additionally, noise regulations have led to offering engines with higher bypass ratios and, thus, reduced core flow. This leads to reduced engine core flow minimum Reynolds numbers. Furthermore, in recent years there has been a strong tendency to reduce the number of blades and stages within aircraft turbomachinery. Thus, the remaining blades are more highly loaded. The increased loading tends to exacerbate low-Reynolds–number effects, extending the portion of the airfoil surface over which boundary layer flow is transitional and/or mildly separated. The combination of all these various effects has led to strong

Manuscript Received on September 17, 2003

interest, recently, in improving the prediction of low Reynolds number flows through Low-Pressure Turbines (LPT).

RECENT RESEARCH AND DEVELOPMENT

The following gives a snapshot of recent research activity related to micro- and small-size engines. Most of the discussion comes from recent International Gas Turbine Conferences (IGTC). Some is a review of research results from our laboratory.

Microturbine systems

The following discusses recent advancements in microturbine system development. Takase et al. (2002) evaluated larger (300kW) microturbine systems that operate at higher pressure ratios as a more economical alternative to the smaller-size, present microturbines. The analysis factored in the lower cost of the recuperator due to lower supply temperatures of the system. Elmegaard and Qvale (2002) studied an Indirectly Fired Gas Turbine (IFGT) fueled with wet biomass. An integrated system was proposed in which the microturbine and the fuel drying system are combined. Analyses of microturbine systems for electric power generation, heating and cooling were presented by Campanari et al. (2002). Various plant schemes and heat pump/chiller systems were considered.

Hybrid fuel cell and microturbine systems were assessed by Bohn et al. (2002). Optimized combined systems and stand-alone operation of a fuel cell or a microturbine were addressed. Kimijima and Kasagi (2002) reviewed their experiences with a gas turbine/fuel cell system. Because of part-load operation during their operational cycle, they found that it was more efficient to run the turbine under variable rotation operation even though the turbomachinery components were at times operating off-design. Development of a combined fuel cell and microturbine at Siemens-Westinghouse was discussed by Veyo et al. (2002). Three sizes were being developed, ranging from 200kW to 500kW. A greater efficiency is gained when the system is used for CHP. Off-design performance of a fuel cell/microturbine system was discussed by Bedont et al. (2002). Particular emphasis was put on CO_2 recycle control. A model used for such assessment was presented. Also, models were presented for fuel cell/microturbine systems by Magistri et al. (2002).

In comparing high-efficiency distributed cogeneration and large-scale, combined-cycle power generation, Martin (2003) concluded that high-efficiency, distributed cogeneration is substantially more energy efficient and economical than large, remote, combined-cycle power plants. Medrano et al. (2003) estimated air quality impact for a representative Distributed Generation (DG) scenario of the year 2010 with comparison to a base case scenario with no DG emissions. A three-dimensional air quality model including detailed atmospheric chemistry and transport was employed.

McDonell et al. (2003) collected operational data from microturbine generators and discussed optimal operational conditions. Isomura et al. (2003) discussed their micro-turbochargers and micro-combustor developments in support of the microturbine system evolution. Performance changes in the development of microturbines due to scaling effects and system configuration were discussed. A conjugate analysis of a turbo charger, including the compressor, the oil-cooled center housing, and the turbine was performed by Bohn et al. (2003a). It was shown that heat transfer from the turbine into the compressor significantly influences the process. Some generalization of heat transfer laws was provided to enable prediction of heat transfer at other operating points with similar geometries. Bohn et al. (2003b) measured temperature distributions on the surfaces of the turbine, compressor and bearing casing. The analysis showed the strong effect of turbine inlet temperature. Bozza et al. (2003) examined possibilities for micro-gas turbine operation under a wide range of thermal and mechanical load requirements. Attention was focused on a partially recuperated thermal cycle based on a bypass option with the heat recovery boiler. They noted the importance of combustor geometry on operation.

Traverso et al. (2003a) discussed transient behavior of two advanced cycles; the Externally Fired micro Gas Turbine (EFmGT) cycle and a solar Closed Brayton Cycle (CBC). The CBC showed good performance and stability over the entire operating range, even when a fault occurred in the control valves. Traverso et al. (2003b) discussed design and off-design performance of an EFmGT demonstration plant. They showed that there is no “forbidden” part-load, steady-state operating point. Akbari and Müller (2003) enhanced the performance of two small gas turbines (30 kW and 60 kW) by implementing various wave rotor topping cycles.

Ceramics

Important to microturbine development are advancements in ceramics. Mutasim (2002) discussed the various effects of the hot section environment on thermal barrier coating life. DiCarlo et al. (2002) documented progress at NASA-Glenn with their ceramic matrix composites for hot-section components. The effectiveness of certain treatments and detrimental effects of inadvertent carbon were discussed. Shi et al. (2002) discussed progress with the design of ceramic axial vane rings and axial turbine rotors for their microturbine. Cox et al. (2002) developed integrally-formed ceramic matrix composite structures for hot-section structures that may be used with active cooling. Fukudome et al. (2002) addressed the problem of recession of Si-based ceramics and evaluated Environmental Barrier Coatings (EBC) for application to hot section components. Miriyala et al. (2002) reviewed test results with Fiber-reinforced Ceramic Composite (CFCC) combustor liners with Environmental Barrier Coatings (EBC). van Roode et al. (2002) discussed impact tests to be applied to ceramic components and noted good performance with CFCC. Sun et al. (2002) also discussed the application of EBCs to silicon nitrite and silicon carbide materials. Lee (2002) proposed EBC applications with a silicon bond coat, an yttria-stabilized zirconia top coat and various intermediate coats. Ellingson et al. (2002) reviewed lower-cost, x-ray, Non-Destructive Evaluations (NDE) of ceramic components for application to the microturbine market. Cost saving is by rejection of poor ceramic pieces before machining time is invested. Walsh et al. (2002) introduced the use of polymer-derived-ceramics (PDC) for fabrication by micro-stereolithography of turbine and recuperator sections. Good stability of the fabricated parts was cited. This is important for the turbine if tip gap clearances are to be maintained.

Carruthers et al. (2002) discussed methods to achieve improved fracture toughness, strength and high temperature environmental resistance of silicon nitride for rotating components. Fett et al. (2002) discussed fracture testing by loading with opposed and concentrated forces via rollers. Stress solutions and intensity factors were presented. Choi et al. (2002) developed a technique for interrogating processes in the zone head of a crack tip, called the frontal zone processes, to assess the relationship between critical size of that zone and fracture toughness and tensile strength.

Jimenez et al. (2003) discussed improving stationary gas turbines in cogeneration plants through selective replacement of hot section metallic components with ceramic components. Fujiwara et al. (2003) introduced research on unique ceramic materials produced through unidirectional solidification with eutectic compositions of two-phase oxides. This material, Melt Growth Composite (MGC), could sustain its room temperature strength up to 1700°C while offering strong oxidization-resistance. Bharadwaj et al. (2003) reported studies on synthesis and oxidation behavior of polymer-derived SiAlCN material, a new class of material synthesized by thermal decomposition of polymeric precursors. Oxidation studies revealed that SiAlCN possesses a lower oxidation rate than SiCN. It was believed that the better oxidation resistance of SiAlCN was due to the oxide

layer containing Al, which slowed oxygen diffusion relative to that with pure SiO_2. Göring et al. (2003) introduced WHIPOX (Wound Highly Porous Oxide CMCs) oxide/oxide composites which are composed of highly porous alumina silicate or alumina fibers. Compared to other long-fiber reinforced ceramic composites, fabrication is cost effective. Non-brittle fracture behavior and mechanical properties are favorable for many technical applications.

Choi et al. (2003) investigated Foreign Object Damage (FOD) behavior with two commercial gas turbine grade silicon nitride composites, AS800 and SN282. Testing was with thin disks impacted by steel-ball projectiles at ambient temperature. AS800 silicon nitride exhibited a greater FOD resistance than SN282, primarily due to its greater fracture toughness. Yuri and Hisamatsu (2003) measured the influence of combustion gas flow conditions on the recession rate of silicon nitride, silicon carbide and alumina, developing a recession rate equation.

Nair and Sun (2003) showed strength and toughness of an Environmental Barrier Coating (EBC)-substrate interface over a wide temperature range. A substantial decrease in the moduli of the EBC coated layers, as well as a decrease in both the strength and toughness of the EBC/substrate interface at elevated temperature were noted. Lin et al. (2003) evaluated the effect of thin CVD-mullite coatings on the mechanical reliability and lifetime performance of SN88 subjected to mechanical loading conditions. Mechanical testing results and SEM examinations indicated that the CVD-mullite coating could not protect the SN88 to ensure long-term mechanical performance and lifetime in gas turbine environments. Durability of liners is limited primarily by the long-term stability of SiC in the high steam environment of the gas turbine combustor. Kimmel et al. (2003) developed an EBC to meet the 30,000-hour life goal. Results of their evaluation from an engine test of greater than 15,000-hours were compared against results of a previous engine test of 14,000-hours. More et al. (2003) conducted high-sample-throughput, first-stage evaluations of EBCs with small ceramic specimens under a range of temperatures, pressures and H_2O concentrations.

Bouillon et al. (2003) tested nozzles made by C-fiber and SiC-fiber CMCs under accelerated conditions without damage for 600 and 1000 hours, respectively. Both materials showed strong potential for improving durability.

Combustors

Because of the slightly non-traditional duty seen by microturbine combustors, we include a discussion of recent microturbine-related combustor developments.

Liedtke et al. (2002) reviewed recent work at Karlsruhe on a counter-flow combustor designed for microturbine application. The concept employs film evaporation of fuel on the hot inner surface of a premix tube to reduce the combustor size. The concept of premixing air and Lower Calorific Value (LCV) gas within the compressor was proposed by van der Wel et al. (2002) to eliminate stall or surge at the operating point, which may arise when air and LCV gas are introduced to the combustor. The effect is tied to the mass flow rate imbalance between the turbine and the compressor when LCV fuel is used. Liedtke et al. (2003) described emission performance of a newly designed liquid fuelled microturbine combustor in which lean premixed pre-vaporized combustion was utilized. Fuel evaporates as a film on the hot inner surface of a premix tube. The heat for evaporation is provided by the outer, counter-flow, hot exhaust gases. To establish almost adiabatic conditions within the reaction zone, the flame tube was designed with a multi-layered geometry, consisting of ceramic rings forming the inner wall, a compliant layer of insulation and the outer metal casing. They investigated the impact of combustor loading, equivalence ratio, staging and ratio between calculated reaction times and mean residence times on the formation of pollutant emissions. They found great potential for pollutant reduction. A low-NOx, high-stability flame combustor was proposed for microturbine application by Shiotani et al. (2002). A swirl zone for ensuring flame stability and a premixing scheme were described.

Rokke et al. (2003) developed a novel 3 MW gas turbine mainly for marine propulsion. It included a dual-fuel, dry low emission (DLE) combustion system designed for single-digit NOx emission. Techniques, such as flame temperature control, staged combustion, lean premixing and lean prevaporized premixing and rich-quench-lean-burning and catalytic combustion were reviewed. Giulio et al. (2003) assessed approaches for numerical simulation of premixed combustion for microturbine design. A flamelet concept routine by N. Peters was employed.

To improve the energy conversion of biomass to electricity, Bohn and Lepers (2003) suggested integration of a micro gas turbine with a biogas generator that allowed more efficient biomass conversion and an extension of biomass digestion to biomasses with reduced biochemical availability. Chiesa et al. (2003) addressed burning hydrogen in a large size, heavy-duty gas turbine designed to run on natural gas. Moderate efficiency reductions were predicted with elevated dilution rates. Cerri et al. (2003) surveyed CO_2 and NOx emission-free hydrogen-fuelled power cycles. They concluded that solutions were needed for turbine operation at the unexplored steam thermodynamic states that would exist in the expansion path. A turbine layout, based on a Ljungström-type radial flow turbine arrangement with massive cooling was presented.

Recuperators

Unique to the microturbine system is integral recuperation. Successful development of cost-effective recuperators is important to the competitiveness of microturbine systems. For this reason, we review recent progress on recuperator development.

A method for evaluating candidate materials for advanced microturbine recuperators, including a means for accelerating the test period, was presented by Lara-Curzio et al. (2002). Lagerström and Xie (2002) described a laser-welded recuperator for microturbine operation. The manufacturing technologies of stamping and laser welding were to reduce the cost of the recuperator and the microturbine system. In a similar paper, Proeschel (2002) presented a recuperator design that was simplified for manufacturing by utilization of welded standard commercial tubing. Antoine and Prieels (2002) presented durability test results on their spiral regenerator design concept. Similarly, Treece et al. (2002) discussed operational results for their recuperator design. Carman et al. (2002) proposed a ceramic microchannel heat exchanger fabricated with micro-stereolithography techniques for application to microturbine regeneration. Pint et al. (2002) discussed the effects of water vapor in the exhaust stream on recuperator materials. With the proposed alloys, the effects were small.

Chapman (2003) utilized laminar flow theory to investigate the effect of heat transfer surface selection, passage size and flow length in compact recuperator design. A simple rectangular flow passage was recommended as a good choice; the flow length should be as small as practical. Kang and McKeiman (2003) designed a new annular type primary surface recuperator for a 200 kW microturbine. It was assembled with a microturbine engine and tested. The design goals of 90% effectiveness and 2.5% total relative pressure drop were achieved. Wilson (2003) explained the principle of operation of regenerative heat exchangers and compared the characteristics with those of recuperators. Implementation of regenerative heat exchangers in current microturbines would improve design-point thermal efficiency and off-design performance. Kesseli et al. (2003) evaluated the performance and economics of recuperation for a practical range of effectiveness values with typical pressure-loss fractions. They showed the strong correlation between recuperator cost and engine specific-power.

Pint and Peraldi (2003) studied oxidation behavior of model alloys to show the alloy composition effects on corrosion resistance of stainless steel components used in recuperators. Better corrosion resistance than with type 347 stainless steel was shown with the composition range of Cr and Ni contents they identified. Finer-grained alloys showed better corrosion resistance than did coarse-grained alloys. Minor alloy additions of Mn and Si are beneficial to corrosion resistance. Maziasz et al. (2003) summarized high-temperature creep and corrosion testing of commercial 347 steel used for recuperators, testing of HR 120 and modified 803 alloys and development of modified 347 stainless steel. A group of cost effective alloys with improved aging, creep and oxidation/corrosion resistance over that of standard 347 austenitic stainless steel was identified.

Turbomachinery

Microturbine development has led to increased development of radial-flow compressors and turbines and small axial-flow turbines. Thus, we review recent developments in these areas of turbomachinery.

Methods for a unified design of radial flow turbomachinery were presented by Ebaid et al. (2002). An optimization procedure was developed to determine the principal dimensions of the rotor. A 3-D, inverse design method was discussed by Zangeneh et al. (2002) for the design of a centrifugal compressor vaned diffuser. The performance of a compressor designed with this method was compared to one designed conventionally. A fully 3-D viscous, turbulent and time-accurate numerical simulation of a centrifugal compressor was presented by Turunen-Saaresti et al. (2002). Computed circumferential variations of total and static pressures were compared to data. Cui (2002) simulated a compressor and evaluated the effects of an elbow upstream of the impeller. The propagation of the inlet non-uniformity into and through the impeller was described. Biba (2002) computed the difference between a constant-area collector design and a volute. The computed results with the collector were compared with experiments. Little difference was found at the design point, but at 115% of design flow, the volute created a 2.5% drop in performance. Mukkavilli et al. (2002) discussed the effects of solidity on the performance of centrifugal machine diffusers. They compared the performance of various designs against the performance of a vaneless diffuser. Off-design performance characteristics of a channel-wedge vaned diffuser, Oh (2002a), and a low-solidity cascade diffuser, Oh (2002b), were investigated by experimentation and computation. Optimum solidity values were proposed and secondary flow fields were discussed. Ferrara et al. measured the effects of the diffuser geometry on rotating stall inception (2002a) and on stage performance (2002b). The working range was strongly influenced by the diffuser design. Bonaiuti et al. (2002) computed secondary flow fields in a low-solidity diffuser. Reasons for stall inception were identified. Time resolved calculations showed the importance of unsteadiness of the flow. Unsteady flow from a centrifugal compressor wheel entering a fishtail diffuser was measured by Yaras and Orsi (2002). At lower frequencies, the unsteadiness had a substantial impact on pressure recovery performance. They noted the importance of unsteadiness and streamline curvature in the strongly-curved fishtail diffuser design. Neither effect was captured well with Reynolds stress turbulence closure models. Plafreyman and Martinez-Botas (2002) computed flow in a mixed-flow turbine and compared the results to experiments taken at their institution. Secondary flows were discussed; tip leakage secondary flows were dominant. Considerable loss was concentrated near the blade leading edge tip region along the full length of the pitch. This was associated with the increased streamline curvature in the meridional plane of the mixed-flow turbine. Ibaraki et al. (2002) conducted detailed experiments on a transonic impeller of a high-pressure-ratio compressor. Their measurements documented interaction of the shock wave and the tip leakage vortex at the inducer, and flow distortion downstream.

Sonoda et al. (2003) developed a high-performance compressor airfoil for operation at a low Reynolds number ($Re=1.3x10^5$). Their objective was to improve the performance of the outlet guide vane used in a single, low pressure turbine of a small turbofan engine for business jet aircraft. Two different numerical optimization methods, the Evolution Strategy (ES) and the Multi-Objective Genetic Algorithm (MOGA), were used in a design process minimizing the total pressure loss and deviation angle at the design point. Schreiber et al. (2003) experimentally investigated aerodynamic characteristics of two new airfoils designed by Sonoda et al. and a conventional, controlled-diffusion airfoil. It was confirmed that the two different optimization methods were able to reduce the total pressure losses at design incidence and increase the low-loss incidence range in the positive direction by about 2 - 3 degrees.

Rodgers (2003) provided an overview of radial turbine performance characteristics for small gas turbine applications, including the influences of specific speed, velocity ratio, exit flow coefficient and rotor tip to exducer root diameter ratio.

Benini et al. (2003a, 2003b and 2003c) conducted experimental and numerical investigations on overall performance of a centrifugal compressor of a 100 KW microturbine. The interaction between impeller and diffuser blades on the flow within the diffuser was simulated. They also optimized the diffuser for maximum aerodynamic efficiency and pressure recovery. Kang et al. (2003) developed a micro-scale, high-speed compressor for application in a fist-sized gas turbine generator. The rotor was manufactured as a single turbine/compressor/shaft unit in silicon nitride by the Mold SDM process. Performance testing and CFD simulation were conducted. Krain (2003) reviewed centrifugal compressor developments focusing on selected practical and theoretical examples that pushed the centrifugal compressor from simple, low-efficiency designs to current high-level performance. The importance of improved theoretical tools, rising computer capacity and advanced measurement techniques were noted.

Streamline curvature

The geometry and flow conditions of the blade passage can cause a complex flow governed by centripetal acceleration, streamwise acceleration and enhanced turbulence. The influences of centripetal acceleration via flow curvature on turbulent transport, transition and separation are next reviewed.

Schultz and Volino (2001) discussed the effects of streamline concave curvature on transition to turbulence. They separated each measurement signal into two, one attributable to the laminar portion of a transitional flow and the other for the turbulent part. They observed that curvature effects were visible in both the laminar and the turbulent portions. Concave curvature is destabilizing, leading to a more upstream transition onset.

Schwarz et al. (2002) examined a turbulent boundary layer in the presence of convex curvature of different strengths combined with various degrees of streamwise pressure gradient. Emphasis was on the near-wall layer of the convex wall boundary layer subjected to various streamwise pressure gradients. Their measurements of mean flow and turbulence showed appreciable changes due to curvature, mainly in the outer portion of the boundary layers. Turbulent burst frequency is changed by wall curvature, enhanced by concave curvature and reduced by convex curvature. Brereton and Shih (2001) assessed the ability of a k-ε, two-equation turbulence model to predict flows with shear and an extra rate of strain, such as rotation or streamline curvature. Smith (2003) presented an Explicit Algebraic Stress Model (EASM) which was shown to significantly improve agreement with experimental data in regions of high curvature.

Ligrani and Hedlund (2003) described heat transfer and flow structure in a channel with a straight portion followed by a portion with mild curvature at Dean numbers from 100 to 1084. Different

flow events were observed, including laminar two-dimensional flow, Dean vortex flow, wavy Dean vortex flow, splitting and merging of Dean vortex pairs, transitional flow with arrays of Dean vortex pairs and fully turbulent flow with arrays of Dean vortex pairs. The Nusselt number varies with curvature, streamwise development and Dean number and is affected by these differently for laminar, transitional and turbulent flows.

Streamline curvature - University of Minnesota

Curvature effects on turbulent transport and transition to turbulence have been experimentally documented in our lab for the past 22 years. Generally, our measurements confirm that concave curvature has a destabilizing effect that augments turbulent transport whereas convex curvature has the opposite effect. Convex curvature causes a dramatic reduction of the primary Reynolds shear stress in the outer portion of the boundary layer compared to values in a turbulent flow over a flat plate. This is attributed to destruction of large eddies in the stable convex-curved flow. Favorable pressure gradients, when interacting with convex curvature, oppose the wake-enhancing effect of convex curvature but augment its stabilizing effect on turbulent stresses, and transport. On the other hand, adverse pressure gradients enhance the wake strength and counteract stabilizing effects of convex curvature. One of the more recent papers from our work, Kestoras and Simon (1997), discusses the effects of removal of concave curvature under both high and low free-stream turbulence conditions. A boundary layer was allowed to develop on a concave wall then flow onto a downstream flat wall. The test wall static pressure was uniform. Elevated values of turbulent shear stress, $\overline{u'v'}$, and turbulent heat flux, $\overline{v't'}$, in the concave-curved boundary layer turbulent core region were immediately reduced to flat-wall values when destabilizing concave curvature was removed on the downstream flat wall (see Fig. 1). This was more pronounced when freestream turbulence was higher. In a low-turbulence case, Goertler vortices that formed on the concave wall were slow to die on the downstream, flat, recovery wall.

Most of our work focused on the effects of curvature on transition. An example is a review paper by Volino and Simon (1995) in which concave and convex-curved transitional flows were compared to flat wall boundary layers with various levels of freestream turbulence. Values compared were the transition start location, transition length, turbulent spot production rate and intermittency distributions. Trends were clear and consistent with the literature, although a point was made that turbulence length scale documentation in the literature is not sufficient to properly separate length scale effects from turbulence level effects. The program went on to include the effects of streamwise acceleration (Volino and Simon 1997a and b). The effect of acceleration is to stabilize the flow which extends the length of the transition region, even when the free-stream turbulence is elevated. One tool for viewing the behavior of transitional boundary layers is octant analysis. Volino and Simon (1994) applied this technique to see the relative importance of such events as hot ejections and cold sweeps to find fundamental differences between fully turbulent flow and transitional flow. In an attempt to describe the effects of freestream turbulence on transition, Volino and Simon (2000) employed a technique called "transfer function" to show which frequencies within the freestream seem to be amplified by the boundary layer during transition.

LOW REYNOLDS NUMBER EFFECTS; BOUNDARY LAYER SEPARATION AND TRANSITION

Properly designing for boundary layer behavior on surfaces of small axial-flow turbomachines is important to the efficiency of the engine when the Reynolds numbers are low. Under these conditions, separation can lead to significant losses. The strength of separation is dependent on transition from laminar to turbulent flow. Thus, both transition and separation become important. In the following, we first discuss models that have evolved for transition prediction in turbomachinery. We then discuss recent research on transition and low Reynolds number boundary layer behavior. Finally, we present recent University of Minnesota data and their use in supporting the models. This has become a very active research area in the last three years.

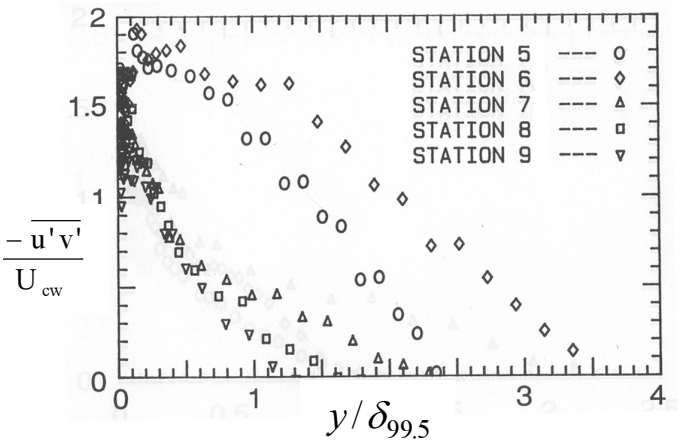

Fig. 1 Turbulent shear stress normalized on U_{cw}, the curved-wall velocity found by exptrapolating the external (inviscid) velicity field to the wall. Staions 5 and 6 are on the concave section whereas stations 7, 8 and 9 are on the flat recovery wall.

NUMERICAL

In recent years, numerical simulations of steady and unsteady transitional flow without, then with, passing wakes have been presented. Most simulations are based on the solution of the Reynolds Averaged Navier-Stokes (RANS) equation in combination with turbulence transport models. Many of these simulations use an algebraic transition modeling in conjunction with an intermittency function to describe how the turbulence term is activated within the transitional flow. Examples of these algebraic models follow.

Determination of transition onset

Separated flow transition. Mayle (1991) developed the following correlation for low free-stream turbulence levels (*TI* = 0.2-0.5%).

$$\mathrm{Re}_{s,st} = 300\,\mathrm{Re}_{\theta,s}^{0.7} \text{ (short bubble)} \quad (1)$$

$$\mathrm{Re}_{s,st} = 1000\,\mathrm{Re}_{\theta,s}^{0.7} \text{ (long bubble)} \quad (2)$$

where $\mathrm{Re}_{s,st}$ is based on the distance from separation to transition onset and $\mathrm{Re}_{\theta,s}$ is based on the momentum thickness at separation.

Roberts (1980) gave the following equations to predict the transition onset:

$$\mathrm{Re}_{s,st} = 25{,}000\log_{10}(\mathrm{Coth}(\mathrm{TF}\times 10)) \quad (3)$$

where $TF = T_{\overline{u}'}(C/L_S)^{1/5}$, C is chord length; L_s is macroscale of the inlet turbulence and $T_{\overline{u}'}$ is inlet turbulence intensity.

Based on Roberts' work, Davis et al. (1985) gave a correlation for the length from the separation point to the transition onset

location in terms of the turbulence level:

$$\mathrm{Re}_{s,st} = 25{,}000 \log_{10}(\mathrm{Coth}(17.32\mathrm{TI_e})) \quad (4)$$

It is presumed that upstream development important to transition is adequately represented by the momentum thickness Reynolds number at separation and the location of separation in the Mayle model and on the local *TI* at separation and the location of separation in the Davis et al. model.

Mayle's separated-flow transition start model will be compared against University of Minnesota data later in this paper.

Attached flow transition. Onset models for attached flow transition are given by Abu-Ghannam and Shaw (1980), Mayle (1991) and Drela (1995). Mayle reviewed research on the effects of free-stream turbulence and pressure gradients on transition onset and gave the following correlation:

$$Re_{\theta,t} = 400TI^{-5/8} \quad (5)$$

Abu-Ghannam and Shaw put a hot-wire probe close to the surface at a fixed chordwise station and increased the tunnel speed gradually until the transition point was at the hot-wire probe location, as indicated by the velocity level. Both start and end of transition were thus identified. Start of transition was taken as the point where the curve showed a rapid rise with increase in flow speed and the end of transition was taken as the peak of the measured velocity vs. flow speed curve. Based on their experiments, and some others, the following correlation for determining transition onset was offered:

$$Re_{\theta,t} = 163 + \exp\left\{F(\lambda_\theta) - \frac{F(\lambda_\theta)}{6.91}TI\right\} \quad (6)$$

where

$$F(\lambda_\theta) = 6.91 + 12.75\lambda_\theta + 63.64(\lambda_\theta)^2 \quad for\ \lambda_\theta < 0$$

$$F(\lambda_\theta) = 6.91 + 2.48\lambda_\theta - 12.27(\lambda_\theta)^2 \quad for\ \lambda_\theta > 0$$

$Re_{\theta,t}$ is the momentum thickness Reynolds number at transition onset and *TI* is free-stream turbulence intensity. Herein, we take this to be at the transition onset location.

Based on the Abu-Ghannam and Shaw model, Drela suggested a correlation that includes the shape factor:

$$Re_{\theta,t} = 155 + 89(0.25\tanh(\frac{10}{H_{12}-1} - 5.5) + 1)\tilde{n}^{1.25} \quad (7)$$

$$\tilde{n} = -8.43 - 2.4\ln(\frac{Tu'}{100}) \quad (8)$$

$$\mathrm{Tu}' = 2.7\tanh\left(\frac{\mathrm{TI}}{2.7}\right) \quad (9)$$

Transition region

In some analyses, only the transition start model is needed and the transitional and turbulent flows are computed with the turbulence model. Others choose to employ transition end and path models to control the means by which the turbulence model is activated. They use the intermittency (the fraction of the flow that is turbulent) to turn on the turbulence term. Transition path models are by Dhawan and Narasimha (1958), Solomon et al. (1996), Boyle and Simon (1998), Ramesh and Hodson (1999) and Schobeiri and Chakka (2002). The last two include the effects of wakes.

It is well known that laminar-to-turbulent transition in a Low-Pressure Turbine (LPT) boundary layer is unsteady and strongly influenced by wakes generated by upstream airfoils. Though great progress has been made toward developing engineering models for steady flow transition, accurate characterization of unsteady transition is in a very early stage of development.

Emmons (1951) introduced the concept of intermittency. The intermittency distribution depends on the rates of formation, propagation and growth of turbulent spots. Emmons assumed that the turbulent spot generation rate was independent of time and position downstream of the onset location. This is called the "continuous breakdown" model. This led to the following equation for intermittency distribution in the transition zone.

$$\gamma = 1 - \exp\left\{-\frac{\sigma}{3U}g(x - x_t)^3\right\} \quad (10)$$

Schubauer and Klebanoff (1955) found disagreement between Emmons' theory and their experimental measurements of intermittency distribution on a flat plate. Narasimha (1957) suggested that turbulent spots are generated only in a narrow region around the transition onset location. This is called the "concentrated breakdown" model. This idea leads to

$$\gamma = 1 - \exp\left\{-\frac{\sigma}{3U}g_n(x - x_t)^2\right\} \quad (11)$$

Intermittency modeling with wakes. Hodson et al. (1992) investigated the intermittency distribution in the transition region in unsteady boundary layer flow under the influence of the wakes, as seen in turbomachinery. They assumed that the wakes could trigger the generation of turbulent spots. As the wakes are traveling, new turbulent spots are generated underneath the wake flow where spots were not being generated prior to the arrival of the wakes. The Ramesh and Hodson (1999) intermittency model 1) incorporates the stabilizing effect of the calmed region behind the turbulent spot and 2) accounts for the effect of fully turbulent fluid inhibiting further spot production. They gave the intermittency distribution as:

$$\gamma = 1 - \exp\left\{-\int_{X_t}^{X}\frac{3G(X_0 - X)^2}{1 + \tau G(X_0 - X_t)^3}dX_0\right\} \quad (12)$$

where γ is intermittency, $X = \frac{Ux}{\nu}$, $X_t = \frac{Ux_t}{\nu}$, $X_0 = \frac{Ux_0}{\nu}$,

$G = \frac{g\sigma\nu^3}{3U^4}$, $\tau = \sigma'/\sigma = 5.44$.

In these expressions, the subscript "t" refers to "at the transition onset point." Also, σ is the spot propagation parameter, σ' is the propagation parameter for spot in the calmed region, τ is the ratio of σ' and σ and *g* is the spot formation rate per unit area per unit time.

In Jiang and Simon (2003b), a relationship between *g* and g_n is developed, where g is the turbulent spot generation rate from the "continuous breakdown" model, Eq. (10), and g_n is for the "concentrated breakdown" model, Eq. (11).

$$0.4549\left(\frac{3U}{g\sigma}\right)^{1/3} = 0.641\left(\frac{U}{g_n\sigma}\right)^{1/2} \quad (13)$$

This allows using g_n from the literature to determine *g* in the above model. Note a different set of units for *g* vs. g_n where g_n is the spot formation rate per unit distance per unit time.

Gostelow et al. (1994) gave a correlation between the spot formation rate, *N*, the pressure gradient parameter, λ_θ, and the freestream turbulence level, *TI*, at the transition onset location as:

$$N = \frac{0.86}{1000}\exp[2.134\lambda_\theta \ln(TI) - 59.23\lambda_\theta - 0.5641\ln(TI)] \quad (14)$$

where $N = \frac{g_n \sigma \theta_t^3}{\nu}$, $\lambda_{\theta_t} = \frac{\theta_t^2}{\nu}\frac{dU}{dx}$, θ_t is the momentum thickness at the transition onset point. The value of σ is in the range 0.25-0.29, as suggested by Narasimha (1985). Hodson took it as 0.25. Thus, we use Eq. (14) to calculate *N*, from which we can get g_n. Then using Eq. (13), we calculate *g* and then *G*, through its definition. Finally, we use Eq. (12) to calculate γ. This form of the intermittency model is applied against the Minnesota data later in this paper.

The effective total diffusivity in the transitional flow is often computed as:

$$\nu_{eff} = \nu_L + \gamma \nu_T \tag{15}$$

where ν_L and ν_T are the molecular and turbulent viscosities, respectively.

Roach and Brierley (2000) presented a model for transition which included both freestream turbulence and turbulence length scale effects. Though the turbulence level is most important, they note the importance of scale in their modeling.

In preparation for further improvements to the intermittency modeling, Gostelow's group experimentally documented spot behavior in strong adverse pressure gradients (D'Ovidio et al. 2001a and b). They added wakes to their experimental program and investigated transition in a separated flow (Gostelow and Thomas, 2003). They found that the calmed region behind a turbulent zone is stronger behind a rod-generated wake than that behind a naturally-occurring spot. Chong and Zhong (2003) studied spot growth on a flat plate with zero and favorable pressure gradients. They recorded the behavior of the overhang of the developing turbulent spot and used the results in their discussion of spot growth.

Simulations with Reynolds-Averaged Navier-Stokes (RANS)

Schobeiri et al. (1998), Chakka and Schobeiri (1999) and Schobeiri and Chakka (2002) used mixing length theory combined with intermittency and the RANS equations to get time-averaged predictions of flow and heat transfer. Computed heat transfer and velocity distributions on the suction surface were compared with measurements.

Kim and Crawford (1998 and 2000) simulated the wake-affected transitional flow on a flat plate. An algebraic turbulence model developed by Cebeci and Smith (1974) was used for the estimation of turbulent viscosity. The empirical correlation of Abu-Ghannam and Shaw (1980) was used to determine the transition onset. The path model was by Hodson et al. (1992).

Chernobrovkin and Lakshminarayana (2000) used the Navier-Stokes code developed by Lakshminarayana et al. (2000) to simulate unsteady flow in a turbine rotor due to nozzle wake-rotor interaction. The predicted flow field was in good agreement with the experimental data at design and off-design conditions. An assessment of viscous and inviscid contributions to nozzle wake decay and unsteady loss distribution in a rotor passage revealed the dominant effect of viscous decay upstream of the leading edge. Inside the passage, inviscid effects (chopping, stretching, distortion, area changes, etc.) had a significant influence. The numerical solver predicted most of the features associated with unsteady transition on a turbine blade.

Eulitz and Engel (1998) used the Reynolds-averaged Navier-Stokes equations together with the Spalart and Allmaras one-equation turbulence model (Spalart and Allmaras, 1992) to investigate wake/blade row interaction in a low-pressure turbine. Transition onset was determined by the Drela (1995) model. The simulation captured separated-flow and wake-induced transition. Instantaneous Mach number and eddy-viscosity plots were utilized to monitor wake migration and interaction with downstream boundary layers. With the same model of Eulitz and Engel (1998), Höhn and Heinig (2000) and Höhn et al. (2001) computed flows with wakes. Unsteady quantities, such as surface pressure, vorticity in the blade passage, unsteady velocity fields and skin friction, were compared with the experiments of Gombert and Höhn (2001). Nayeri and Höhn (2003) used a Navier-Stokes solver with the Spalart-Allmaras one-equation turbulence model and the Drela (1995) transition onset model to compute flow over a three-stage low pressure turbine. They noted a need for adjustment of parameters in the turbulence and transition models and suggested that more work is needed to find the proper parameters to be used for this adjustment. Hu and Fransson (2000) compared three transition models in an industrial Navier-Stokes solver. They noted that the accuracy of prediction depends on flow conditions. Generally, however, the e^N model of transition was more successful in the presence of a strong adverse pressure gradient. Suzen et al. (2000) computed the flow of Qiu (1996), Qiu and Simon (1997) and Simon et al. (2000) using a transport equation for intermittency, the Roberts (1980) separated flow transition onset model and the Abu-Ghannam and Shaw (1980) attached flow onset model to successfully match the data over a range of Reynolds numbers and turbulence intensity values. They later expanded their test cases to include three LPT test cases (Suzen et al., 2003). Suzen and Huang (2003) next moved to a simulation of the unsteady data with bar-generated wakes of Kaszeta et al. (2001) and Schobeiri and Pappu (1997). In this case, they used a turbulence model without transition modeling. They noted a need to take transition into consideration in the analysis. Lodefier et al. (2003) used a two-equation, k-ω model with a dynamic intermittency model for simulation of flat plate and cascade boundary layer transition. Onset was based upon local quantities. The model was developed with the flat plate data and verified in the cascade.

Gier et al. (2000) performed a steady, 3-D flow simulation using a modified Abu-Ghannam and Shah transition model and a two-equation turbulence closure model. Their comparisons with data indicated a need for improved transition onset modeling.

Cardamone et al. (2002) computed the effects of wakes on boundary layer transition in a highly loaded, axial-flow, Low Pressure Turbine (LPT). The flow had a large separation bubble on the suction surface. For turbulence closure, they used the Spalart-Allmaras model and for transition onset they used Drela's formulation of the Abu-Ghannam and Shaw model. For the higher Reynolds number case, predictions were good, with a noted exception that the effects of the calmed region that follows the passage of a turbulent spot was over-predicted. For the low-Reynolds-number case with massive separation, the comparison of model results and experimental data showed large discrepancies. The computed losses were much larger and the separation streamline was computed to not reattach. Clearly, transition was predicted to proceed too slowly. Vicedo et al. (2003) presented a separated flow intermittency model which includes the effects of entrainment of surrounding fluid, then used it with the Mayle onset model to verify its performance against a well-established test case. Work by the same group (Vilmin et al. 2003) used a CFD solver with the Abu-Ghannam and Shaw transition model. They showed that they could resolve the transient features in the separated flow under the wake as identified in their experimental data from a high-lift LPT airfoil experiment.

Researchers at VKI and Snecma investigated the effects of wakes on transition in a high-lift LPT. They conducted experiments with rotating bars (Coton et al., 2002) and made CFD simulations of the experiments (Roux et al. 2002). For transition onset, the Drela scheme was used for attached flow and the Davis scheme was employed for separated flow transition. The transition length was computed with a model by Solomon et al. (1996). Changes of static pressure distribution and turbulence, both associated with oncoming wakes, were important. The choice of the numerical spatial scheme was shown to be important in the prediction of transition onset. Comparisons with heat transfer results indicated that an improved turbulence model and

an improved transition model that incorporate wakes are needed. They later presented satisfactory results (Houtermans et al. 2003) for analysis of a highly-loaded LPT with the laminar flow, separated flow transition model they developed.

Thurso and Stoffel (2001) applied linear and non-linear, low-Reynolds-number, k-ε, eddy viscosity models to the numerical simulation of unsteady wake effects on transition, as induced by separation and wake passing turbulence. Although the models couldn't capture the details of the dynamic features of the separation bubble under unsteady flow conditions, they could reproduce relevant unsteady flow phenomena, e.g. the velocity oscillation effects on the bubble length. The models over-predicted transition length and showed deficiencies with respect to skin friction coefficient distribution in the fully-turbulent flow region when they were used to simulate transition, as triggered by passing wakes.

Liu et al. (2002) studied bypass transition in separated flow within the LPT to assess transition modeling. The CFD results were compared to rig data. Though the separation location was poorly predicted, the effects of decreasing Reynolds numbers on airfoil overall performance were predicted well. Sanz and Platzer (2002) studied the effects of transition models and solution methods on computed transition behavior. They found that such parameters as discretization scheme of the turbulence model or the flow solver have a large influence on computational results, comparable to those of the choice of transition model. Using a three-dimensional Navier-Stokes code, Roux et al. (2001) investigated the effects of choice of transition and turbulence models, free stream turbulence (on laminar boundary layers) and mesh refinement. An analysis of a transitional boundary layer was presented by Palma (2002). For turbulence closure, the k-ω model was used and for transition, the Mayle separated-flow transition onset model was employed. Computed results were found to be fair when compared to data from an LPT cascade and from a transonic-flow compressor cascade. Stadtmuller et al. (2000) used the unsteady boundary layer interaction method to compute wall shear stresses on the suction surface of an LPT, as affected by passing wakes. Their results compared favorably with their measurements.

Direct Numerical Simulation (DNS)

Wu and Durbin (2000) performed DNS of unsteady wake effects and of transition on a flat plate and in a turbine passage. The development of wakes in a low-pressure turbine passage and bypass transition on a zero pressure gradient flat plate were also simulated and presented. They compared the DNS prediction of transition induced by periodic wakes to those of RANS methods, e.g. the Spalart and Allmaras one-equation turbulence model and the v^2-f model. The gross features of the transitional flow were predicted.

Other efforts

Walters and Leylek (2003a) used a commercially-available solver and a three-equation, eddy-viscosity model developed by them to resolve unsteady transition due to passing wakes. They found an improvement over RANS-based modeling. They showed success of the model when applied to highly-loaded cascade airfoils (2003b). Victor and Houdeville (2000) divided the boundary layer into two regions. In the near-wall region, the mixing length with the Van Driest wall damping function was used; in the region away from the wall (y^+>75), the k-ε model was used. The velocity profile and the shape parameters from predictions were compared with experiments. Good agreement of phase-averaged velocity and shape parameter was found.

Johnson (2002) utilized linear perturbation methods to predict receptivity of a laminar boundary layer to freestream turbulence consisting of vortex arrays. His method predicted the growth of fluctuations in the laminar boundary layer as initiated by the freestream turbulence intensity and as influenced by the freestream turbulence length scale. Hence, his method could determine the start of transition without empirical correlation. Johnson (2003) used this analysis to compute the receptivity of boundary layers to freestream turbulence for various pressure gradients. This method computed transition onset values that were in agreement with the Abu-Ghannam and Shaw correlation.

EXPERIMENTAL

Because transitional flows are not well understood, experimental work is important. Recent work which pertains to the LPT is reviewed next.

Volino and Hultgren (2000) studied separated flow transition on a flat plate with an imposed pressure gradient that simulated that of an LPT. They described the effect of freestream turbulence on the instability in the shear layer of the separation bubble. Schultz and Volino (2001) discussed the effects of combined streamline concave curvature and streamwise acceleration on transition to turbulence. Both effects were shown to be important. Volino (2002a) documented the changing scales of velocity fluctuation in a boundary layer passing through transition by using wavelet spectral analysis. Self-similarity of the turbulent zone was found. In the non-turbulent zone, the dominant frequencies were those of the free-stream. Volino (2002b and 2002c) discussed measurements in separated-flow transition under LPT conditions with various Reynolds numbers and free stream turbulence intensity values. Mean and fluctuating velocity profiles, turbulent shear stress profiles and intermittency profiles were presented. From power spectral distributions, transition was identified by a sharp peak in the spectra when the freestream turbulence level was low and a broad band of turbulence when the free-stream turbulence was elevated. Volino et al. (2001) applied conditional sampling against data from a transitional boundary layer subject to high (initially 9%) free-stream turbulence and strong acceleration to separate the turbulent and non-turbulent zone data. They found that mean velocity profiles were clearly different in the turbulent and non-turbulent zones and skin friction coefficients were as much as 70% higher in the turbulent zone. Eddy transport in the non-turbulent zone is significant, however, and the non-turbulent zone does not behave like a laminar boundary layer. Within each of the two zones there was considerable self-similarity of the mean profiles from the beginning to the end of transition, each behaving like their respective fully developed flows. This may prove useful for future modeling efforts.

Yaras (2001) suggested that separation bubble transition occurs at a local pressure gradient that differs significantly from the upstream pressure profile. In the case of low free-stream disturbances, development of instability waves prior to separation changed as upstream history changed. Measurements documented the effects of such pressure gradients on the separated region transition process. Yaras (2002) continued such measurements and discussed the effects of pressure waves prior to separation. In 2003, Roberts and Yaras measured transition behavior in attached-flow (2003a) and separated-flow (2003b). Their measurements were used to assess existing models for transition and to support development of an attached flow transition length model. Volino and Murawski (2003) experimentally documented transitional boundary layer flow in a cascade, measuring mean velocity profiles and turbulence, including spectra. They note that small but measurable differences in the spectra of the low free-stream turbulence cases can have a significant effect on boundary layer reattachment.

Lou and Hourmouziadis (2000) experimentally documented unsteady separation bubbles in a flat plate flow with an opposite wall that is contoured to create a pressure profile of an LPT and flow pulsation to simulate the unsteadiness of passing wakes. They identified characteristic instability frequencies in the free shear layer. Solomon (2000) took surface pseudo shear stress measurements in a rotating, two-stage turbine to investigate the

effects of wakes and loading. He reduced the solidity and increased the loading in comparison cases to observe separated flow transition. He noted that if the upstream blade rows were properly clocked, he could completely eliminate the periodicity of the wake induced transition. Brunner et al. (2000) used results of an experiment with moving bar-generated wakes to show that the LPT could be redesigned for higher loading if the effects of rotor-stator interaction were incorporated into the design. In a companion paper, these researchers presented multi-sensor hot wire measurements to describe the boundary layer flow on a highly loaded LPT (Wolff et al. 2000) and in a third paper from the same group (Teusch et al. 2000), they presented measurements of boundary layer development and losses as affected by incoming wakes. The wakes induce earlier transition, reducing the separation bubble size and the losses associated with separation. Howell et at. (2001) measured unsteady boundary layer behavior in two, high-lift and one, ultra-high-lift LP turbines using surface-mounted hot-film sensors. Regions of wake-induced transition, natural transition and calming in the boundary layer were identified and effects of passing wakes on these regions were discussed. Funazaki and Aoyama (2000) measured Reynolds shear stress distributions in the wake-affected boundary layer to show clearly such transport in the calmed region. Funazaki et al. (2003) used similar measurements to experimentally describe the effects of wakes on leading edge separation bubbles. They note the strong effects of wakes and subsequent calmed regions on separation zone size. Stieger and Hodson (2003) measured the effects of wakes on separated flow transition, noting the creation of an inflectional profile due to the wake and the development of inviscid Kelvin-Helmholtz rollup of the shear layer, leading to transition. They also documented pressure changes with passing wakes (Stieger et al. 2003) and tied the pressure response to coherent vortices that form in the boundary layer as the wakes pass. In a similar study, Jiang and Simon (2003c), documented the effect of the spatial and temporal acceleration fields, as affected by passing wakes, on transition of the flow over an LPT. They also varied the wake spacing and the background turbulence intensity (Kaszeta et al. 2003) to show the effect of each on transition in the wake-affected flow on the LPT suction surface. The case with decreased wake spacing allowed a more detailed look at the calming effect after the passing of a wake. Radomsky and Thole (2001) examined the effects of elevated freestream turbulence levels on boundary layer development along a stator vane airfoil. Both the mean and fluctuating velocities on the pressure and suction surfaces were measured by using a two-component LDV system. Schobeiri et al. (2003) measured unsteady boundary layer behavior as influenced by rod-generated wakes. Measurements over a Reynolds number range from 50,000 to 125,000 allowed a description of the onset and extent of separation and transition zones.

Several studies developed means for control over transition. Byerley et al. (2002) showed that a Gurney flap on the downstream pressure surface could eliminate or reduce the suction-surface separation bubble that appears when operating at very low Reynolds numbers. Volino studied the use of rectangular bars (2003a) and issuing jets (2003b) on the suction surface of a low-pressure turbine for control of transition. At low Reynolds numbers, the bars are effective, but they add to the loss at high Reynolds numbers. The jets showed improvement over the non-controlled case and over the passive control case (in which the bars were used). Wang and Rice (2003) looked at the effects of surface roughness and found a more upstream transition on some of their rough surfaces when the turbulence intensity was elevated, but no lasting effects of roughness for cases where the turbulence was low.

Walsh et al. (2002) discussed local entropy generation in transitional boundary layers with freestream pressure gradients, giving a quick and simple method for comparing performance between one design and another.

Low Reynolds number effects and boundary layer transition - the University of Minnesota data

Below, the separated flow transition model of Mayle and the path model of Ramesh and Hodson (1999) are applied against data taken at the University of Minnesota to assess their performance for use on the suction surface of a turbine blade in the presence of passing wakes

The Data with Wakes. Kaszeta (2000), Kaszeta and Simon (2002) and Kaszeta et al. (2001) conducted experiments on the effects of passing wakes on transition of the suction surface boundary layer on a low-pressure, axial-flow turbine. The background (ahead of the wake generator) freestream turbulence intensity, *FSTI,* was 2.5% and the Reynolds number, *Re,* was 50,000 based upon suction surface length and exit velocity. They modified the cascade of Qiu (1996), Qiu and Simon (1997) and Simon et al. (2000) to add wakes generated by rods. Kaszeta collected ensemble-averaged profiles of velocity, turbulence intensity and turbulence intermittency. Ensemble averaging was based upon position within the wake-passing period. The cycle beginning point, $\theta = 0$, is arbitrary.

Figure 2 shows transition onset location from these results compared with Mayle's model (Jiang and Simon 2003a). Included are time-resolved and time-averaged data as well as two steady cases (without wakes) with *TI*=2.5% and *TI*=10%.

For time-resolved data, we see that the points are divided into two parts: (1). points near the long bubble model prediction. ($88° < \theta < 320°$ of the wake-passing cycle) during which transition is at the downstream edge of the suction surface (sometimes slightly beyond the trailing edge, for which we assumed the trailing edge as the transition location). (2). points near the short bubble model prediction ($4° < \theta < 84°$ and $324° < \theta < 360°$ of the wake-passing cycle).

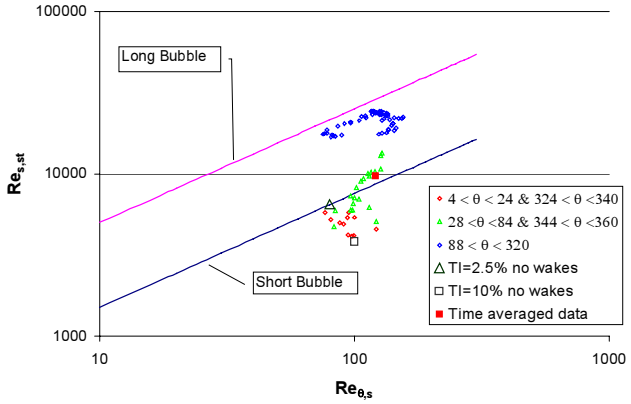

Fig. 2 Mayle's model and the University of Minnesota data

$4° < \theta < 24°$ and $324° < \theta < 340°$. Turbulent strips generated by wakes trigger transition in the near-wall boundary layer. Though no intermittency rise associated with transition is visible in the pre-separation boundary layer flow, wake turbulence has a strong influence in destabilizing the flow. Incipient transition seems to appear far upstream (much earlier than predicted) in the periods from $4° < \theta < 24°$ and from $324° < \theta < 340°$ but doesn't seem to proceed through transition until considerably farther downstream. The point of beginning of "sustained transition" is taken as the onset location.

$28° < \theta < 84°$ and $344° < \theta < 360°$. In these periods, transition onset location moves along with the passing wake. The onset locations are just upstream of these wakes, indicating a short lag between the time at which the wake is nearby and the onset of transition. In this range, flow develops to become fully turbulent

soon after incipient transition occurs, while transition in the range $4° < \theta < 24°$ and $324° < \theta < 340°$ is extended by acceleration.

$88° < \theta < 320°$. In this range, the wake has passed the transition zone, the free stream outside of the boundary layer is temporally accelerated and the effect of acceleration on the boundary layer is to stabilize the flow. Therefore, transition is retarded. But, from the profile of intermittency, we can conclude that transition occurs downstream of the measurement zone, or perhaps downstream of the test section trailing edge. When the latter, we set the transition point to be the airfoil trailing edge.

Often in design, the time-averaged transition location is of interest, but the effects of wakes must be considered. Thus, in this section, we assess whether the correlation for determining the transition point can be used in time-averaged simulations of unsteady flows if the input parameters include the effects of unsteadiness. Figure 2 shows a single time-averaged value of $Re_{s,st}$ vs $Re_{\theta,s}$. The first is computed by averaging the time-resolved separation and transition points to find the cycle-average separation and transition points, then computing $Re_{s,st}$. The second is found by averaging the time-resolved momentum thickness values at separation to compute the time-average momentum thickness value, then computing $Re_{\theta,s}$. We note that had we entered the Mayle correlation with this value of $Re_{\theta,s}$ and had we assumed a short bubble separation behavior, we would have computed a value of $Re_{s,st}$ from the model that is very close to the $Re_{s,st}$ value we computed from the measurements.

Jiang and Simon (2003b) applied the Ramesh and Hodson (1999) path model discussed above to the Minnesota data. They computed $\gamma\left(\theta, x/L_{ss}\right)$ then averaged over θ to get the cycle-average $\gamma\left(x/L_{ss}\right)$ shown in Fig. 3. The predicted γ continues to grow with x/L_{ss}, as the model requires. However, the real flow transitions while the wake is present and recovers after the wake has passed, leading to a leveling of $\gamma\left(x/L_{ss}\right)$ on the aft region.

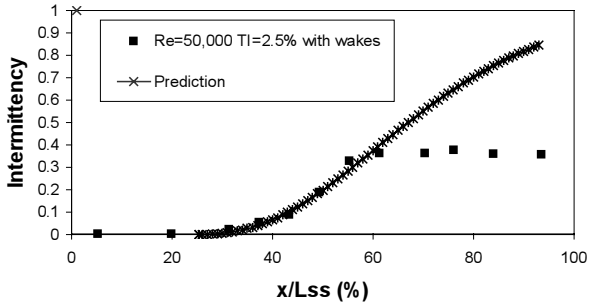

Fig. 3. Comparison of predicted and experimental γ values.

Due to the velocity deficit caused by a passing wake, the free stream to the suction surface boundary layer oscillates during the wake passing cycle. This oscillation causes temporal acceleration and deceleration of the flow. Also, the free stream velocity changes spatially along the suction surface due to the passage geometry. Transition is determined by the total effect of temporal and spatial acceleration, which is the substantial derivative:

$$\frac{D\vec{\mathbf{u}}}{Dt} = \frac{\partial\vec{\mathbf{u}}}{\partial t} + \vec{\mathbf{u}}\nabla\vec{\mathbf{u}} \qquad (16)$$

To show changes in the flow during the wake-passing cycle, we created movies from the Kaszeta data. Figure 4 is one picture from one movie. It shows transition as rising near-wall values of intermittency at *s/Lss*=55-65%, downstream of the throat, while the large intermittency values beyond the boundary layer at *s/Lss*=75-90% represent the passing wake. Note the region of high intermittency values lifting off the wall as the separation zone thickens over the range *s/Lss*=55-80%. A deceleration region occurs at this location, indicated by negative values of *Du/Dt* and $u\partial u/\partial x$. Important to flow separation and transition are temporal acceleration, spatial acceleration and free-stream turbulence, all affected by the passing wakes. The movies help in looking at these effects separately. More discussion is in Jiang and Simon (2003c).

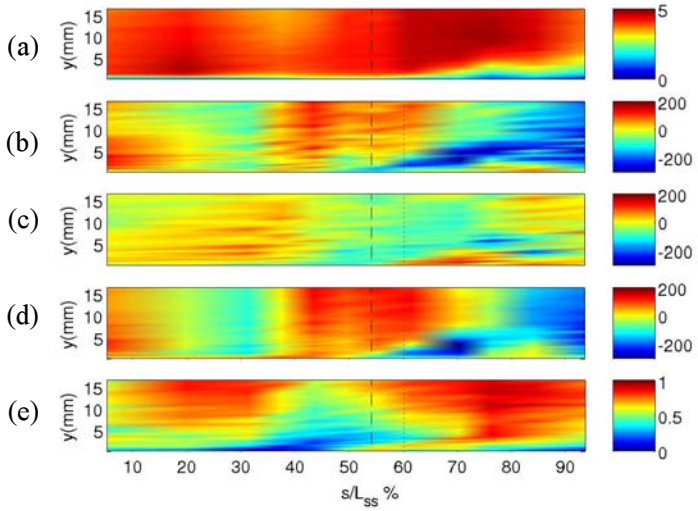

Fig. 4 One picture from one movie ((a) velocity, (b) Du/Dt, (c) $\partial u/\partial t$, (d) $u\partial u/\partial x$, (e) intermittency). This is at θ=320°. Color scale indicates values of the parameter, plotted vs. distance from wall, y(mm), and streamwise distance, s, is normalized on suction surface length, *Lss*. The dashed line is transition onset and the dotted line is separation.

CONCLUSIONS

In this paper, we first discussed recent develops that have raised the interest in microturbine and small turbine engine development. Following this, we reviewed some recent literature in support of microturbine and small turbine development, including streamwise curvature and boundary layer transition. We completed the paper by discussing these two effects in some detail and presented some recent work conducted at the University of Minnesota.

ACKNOWLEDGEMENTS

The University of Minnesota transition work is part of a study of transition in LP turbines sponsored by the NASA Glenn Research Center under cooperative agreement #NCC3-652. The contract monitor is Dr. David Ashpis.

REFERENCES:

MICROTURBINE SYSTEMS

Akbari, P. and Müller, N., 2003, "Performance Improvement of Small Gas Turbines Through Use of Wave Rotor Topping Cycles," ASME paper GT2003-38772.

Bedont, P., Grillo, O. and Massardo, A. F., 2002, "Off-design Performance Analysis of a Hybrid System Based on an Existing MCFC Stack," ASME paper GT-2002-30115.

Bohn, D., Heuer, T. and Kusterer, K., 2003a, "Conjugate Flow and Heat Transfer Investigation of a Turbo Charger: Part I: Numerical Results," ASME paper GT2003-38445.

Bohn, D., Mortiz, N. and Wolff, M., 2003b, "Conjugate Flow and Heat Transfer Investigation of a Turbo Charger: Part II: Experimental Results," ASME paper GT2003-38449.

Bohn, D., Pöppe, N. and Lepers, J., 2002, "Assessment of the Potential of Combined Micro Gas Turbine and High Temperature Fuel Cell Systems," ASME paper GT-2002-30112.

Bozza, F., Cristina, M. and Tuccillo, C. R., 2003, "Adapting the Micro-Gas Turbine Operation to Variable Thermal and Electrical Requirements," ASME paper GT2003-38652.

Campanari, S., Boncompagni, L. and Macchi, E., 2002, "Microturbines and Regeneration: Optimization strategies and Multiple Engine Configuration Effects," ASME GT-2002-30417.

Elmegaard, B. and Qvale, B., 2002, "Analysis of Indirectly Fired Gas Turbine for Wet Biomass Fuels Based on Commercial Micro Gas Turbine Data," ASME paper GT-2002-30016.

Isomura, K., Murayama, M., Yamaguchi, H., Ijichi, N., Saji, N., Shiga, O., Takahashi, K., Tanaka, S., Genda, T. and Esashi, M., 2003, "Development of Micro-Turbo Charger and Micro-Combustor as Feasibility Studies of Three-Dimensional Gas as Turbine at Micro-Scale," ASME paper GT2003-38151.

Kimijima, S. and Kasagi, N., 2002, "Performance Evaluation of Gas Turbine-Fuel Cell Hybrid Micro Generation System," ASME paper GT-2002-30111.

Magistri, L., Bozza, R., Costamagna, P. and Massardo, A. F., 2002, "Simplified Versus Detailed SOFC Reactor Models and Influence on the Simulation of the Design Point Performance of Hybrid Systems," ASME paper GT-2002-30653.

Martin, J. R., 2003, "Comparison of High-Efficiency Distributed Cogeneration and Large Combined-Cycle Power Generation," ASME paper GT2003-38109.

McDonell, V. G., Hack, R. L., Lee, S. W., Mauzey, J. L., Wojciechowski, J. S. and Samuelsen, G. S., 2003, "Experiences with Microturbine Generator Systems Installed in the South Coast Air Quality Management District," ASME paper GT2003-38777.

Medrano, M., Brouwer, J., Samuelsen, G. S., Carreras, M. and Dabdub, D., 2003, "Urban Air Quality Impacts of Distributed Generation," ASME paper GT2003-38309.

Takase, K., Furukawa, H. and Nakano, K., 2002, "A Preliminary Study of an Inter-Cooled and Recuperative Microgasturbine Below 300 kW," ASME paper GT-2002-30403.

Traverso, A., Calzolari, F. and Massardo, A., 2003a, "Transient Analysis and Control System for Advanced Cycles Based on Micro Gas Turbine Technology," ASME GT2003-38269.

Traverso, A., Magistri, L., Scarpellini, R. and Massardo, A., 2003b, "Demonstration Plant and Expected Performance of an Externally Fired Micro Gas Turbine for Distributed Power Generation," ASME paper GT2003-38268.

Veyo, S. E., Litzinger, K. P., Vora, S. D. and Lundberg, W. L., 2002, "Status of Pressurized SOFC/Gas Turbine Power System Development at Siemens Westinghouse," ASME GT-2002-30670.

CERAMICS

Bharadwaj, L., Dhamne, A., An, L., Fookes, B., Kapat, J. and Chow, L., 2003, "Polymer-Derived SI-AL-C-N-O Ceramics for High Temperature Applications," ASME paper GT2003-38561.

Bouillon, E. P., Spriet, P. C., Habarou, G., Arnold, T., Ojard, G. C., Feindel, D. T., Logan, C. P., Rogers, K., Doppes, G., Miller, R. J., Grabowski, Z. and Stetson, D. P., 2003, "Engine Test Experience and Characterization Of Self Sealing Ceramic Matrix Composites For Nozzle Applications in Gas Turbine Engines," ASME paper GT2003-38967.

Carruthers, W. D., Becher, P. F., Ferber, M. K., Roode, M. and Pollinger, J., 2002, "Advances in the Development of Silicon Nitride and Other Ceramics," ASME paper GT-2002-30504.

Choi, S., Okamoto, M. and Awaji, H., 2002, "A Novel Technique for Estimation of Critical Frontal Process Zone Size in Ceramics," ASME paper GT-2002-30508.

Choi, S. R., Pereira, J. M., Janosik, L. A. and Bhatt, R. T., 2003, "Foreign Object Damage of Two Gas-Turbine Grade Silicon Nitrides in a Thin Disk Configuration," ASME GT2003-38544.

Cox, B. N., Davis, J. B., Marshall, D. B. and Yang, Q. D., 2002, "Integral Textile Ceramic Composites for Turbine Engine Combustors," ASME paper GT-2002-30056.

DiCarlo, J. A., Yun, H. M., Morscher, G. N. and Bhatt, R. T., 2002, "Progress in SiC/SiC Ceramic Composite Development for Gas Turbine Hot-Section Components under NASA EPM and UEET Programs," ASME paper GT-2002-30461.

Ellingson, W. A., Koehl, E. R., Stainbrook, J. and Rivers, M., 2002, "Volumetric X-Ray Imaging for Ceramic Microturbine Rotors," ASME paper GT-2002-30549.

Fett, T., Munz, D. and Thun, G., 2002, "Fracture Toughness Testing on Bars under Opposite Cylinder Loading," ASME paper GT-2002-30507.

Fujiwara, K., Nakagawa, N., Kobayashi, K., Yokoi, S., Kihara, T. and Takamatsu, H., 2003, "Research on Application of Melt-Growth Composite Ceramics to Gas Turbines," ASME paper GT2003-38029.

Fukudome, T., Tsuruzono, S., Karasawa, W. and Ichikawa, Y., 2002, "Development and Evaluation of Ceramic Components for Gas Turbine," ASME paper GT-2002-30627.

Göring, J., Kanka, B. and Schneider, M. S. H., 2003, "A Potential Oxide/Oxide Ceramic Matrix Composite for Gas Turbine Applications," ASME paper GT2003-38836.

Jimenez, O., Bagheri, H., McClain, J., Ridler, K. and Bornemisza, T., 2003, "CSGT: Final Design and Test of a Ceramic Hot Section," ASME paper GT2003-38978.

Kimmel, J., Price, J., More, K., Tortorelli, P., Sun, E. and Linsey, G., 2003, "The Evaluation of CFCC Liners after Field Testing in a Gas Turbine – IV," ASME paper GT2003-38920.

Lee, K. N., 2002, "Environmental Barrier Coatings Having a YSZ Top Coat," ASME paper GT-2002-30626.

Lin, H.-T., Ferber, M. K., Kirkland, T. P. and Zemskova, S. M., 2003, "Dynamic Fatigue of CVD-Mullite Coated SN88 Silicon Nitride," ASME paper GT2003-38919.

Miriyala, N., Kimmei, J., Price, J., More, K., Tortorelli, P., Eaton, H., Linsey, G. and Sun, E., 2002, "The Evaluation of CFCC Liners after Field Testing in a Gas Turbine – III," ASME paper GT2002-30585.

More, K. L., Tortorelli, P. F. and Walker, L. R., 2003, "Verification of an EBC's Protective Capability by First-Stage Evaluation in a High Temperature, High-Pressure Furnace," ASME paper GT2003-38923.

Mutasim, Z., 2002, " Intrinsic and Extrinsic Variable Effects on Thermal Barrier Coatings Life," ASME paper GT-2002-30273.

Nair, S. and Sun, E. Y., 2003, "Strength and Toughness of Interface between EBC and Ceramic Substrates at Elevated Temperature," ASME paper GT2003-38918,

Shi, J., Vedula, V. R., Holowczak, J., Bird, C. E. and Ochs, S. S., 2002, "Preliminary Design of Ceramic Components for the ST5+ Advanced Microturbine Engine," ASME GT-2002-30547.

Sun, E. Y., Eaton, H. E., Holowczak, J. E. and Linsey, G. D., 2002, " Development and Evaluation of Environmental Barrier Coatings for Silicon Nitride," ASME paper GT-2002-30628.

van Roode, M., Jimenez, O., McClain, J., Price, J., Poormon, K. L., Parthasarathy, V., Ferber, M. K. and Lin, H., 2002, "Ceramic Gas Turbine Materials Impact Evaluation," ASME paper GT-2002-30505.

Walsh, C., An, L., Kapat, J. S. and Chow, L. C., 2002, "Feasibility of a High-Temperature Polymer-Derived-Ceramic Turbine Fabricated through Micro-Stereolithography," ASME paper GT-2002-30548.

Yuri, I. and Hisamatsu, T., 2003, "Recession Rate Prediction for Ceramic Materials in Combustion Gas Flow," ASME paper GT2003-38886.

COMBUSTOR

Bohn, D. and Lepers, J., 2003, "Effects of Biogas Combustion on the Operation Characteristics and Pollutant Emissions of a Micro Gas Turbine," ASME paper GT2003-38767.

Cerri, G., Battisti, L. and Soraperra, G., 2003, "Non Conventional Turbines for Hydrogen Fueled Power Plants," ASME paper GT2003-38324.

Chiesa, P., Lozza, G. and Mazzocchi, L., 2003, "Using Hydrogen as Gas Turbine Fuel," ASME paper GT2003-38205.

Giulio, G. C., Viatcheslav, M., Anisimov, V. and Parente, J., 2003, "Assessment of Traditional and Flamelets Models for Micro Turbine Combustion Chamber Optimisation," ASME paper GT2003-38385.

Liedtke, O., Schulz, A. and Wittig, S., 2002, "Design Study of a Lean Premixed Prevaporized Counter Flow Combustor for a Micro Gas Turbine," ASME paper GT-2002-30074.

Liedtke, O., Schulz, A. and Wittig, S., 2003, "Emission Performance of a Micro Gas Turbine LPP-Combustor with Fuel Film Evaporation," ASME paper GT2003-38697.

Rokke, P. E., Hustad, J. E., Røkke1, N. A. and Svendsgaard, O. B., 2003, " Technology Update on Gas Turbine Dual Fuel, Dry Low Emission Combustion Systems," ASME GT2003-38112.

Shiotani, H., Takagi, T., Okamoto, T., Kinoshita, S., and Teraoka, H., 2002, "Construction of Low NOx and High Stability Flames Aiming at Micro Gas Turbine Combustion," ASME paper GT-2002-30463.

van der Wel, M.C., Kramer, M. and van Buijtenen, J. P., 2002, "Premixing Air and LCV Gas in a Gas Turbine Compressor," ASME paper GT-2002-30015.

RECUPERATOR

Antoine, H. and Prieels, L., 2002, "The Acte Spiral Recuperator for Gas Turbine Engines," ASME GT-2002-30405.

Carman, B. G., Kapat, J. S., Chow, L. C. and An, L., 2002, "Impact of a Ceramic Microchannel Heat Exchanger on a Micro Turbine," ASME paper GT-2002-30544.

Chapman, W. I., 2003, "Laminar Flow Theory as a Guide to Compact Recuperator Design," ASME paper GT2003-38087.

Kang, Y. and McKeirnan, R., 2003, "Annular Recuperator Development and Performance Test for 200KW Microturbine," ASME paper GT2003-38522.

Kesseli, J., Wolf, T., Nash, J. and Freedman, S., 2003, "Micro, Industrial, and Advanced Gas Turbines Employing Recuperators," ASME paper GT2003-38938.

Lagerström, G. and Xie, M., 2002, "High Performance & Cost Effective Recuperator for Micro-Gas Turbines," ASME paper GT-2002-30402.

Lara-Curzio, E., Maziasz, P. J. and Pint, B. A., 2002, "Test Facility for Screening and Evaluating Candidate Materials for Advanced Microturbine Recuperators," ASME GT-2002-30581.

Maziasz, P. J., Pint, B. A., Swindeman, R. W., More, K. L. and Lara-Curzio, E., 2003, "Selection, Development and Testing of Stainless Steels and Alloys for High-Temperature Recuperator Applications," ASME paper GT2003-38762.

Pint, B. A., More, K. L. and Tortorelli, P. F., 2002, "The Effect of Water Vapor on Oxidation Performance of Alloys Used in Recuperators," ASME paper GT-2002-30543.

Pint, B. A. and Peraldi, R., 2003, "Factors Affecting Corrosion Resistance of Recuperator Alloys," ASME paper GT2003-38692.

Proeschel, R. A., 2002, "Proe 90^{TM} Recuperator for Microtubine Applications," ASME paper GT-2002-30406.

Treece, B., Vessa, P. and Mckeirnan, R., 2002, "Microturbine Recuperator Manufacturing and Operating Experience," ASME paper GT-2002-30404.

Wilson, D. G., 2003, "Regenerative Heat Exchangers for Microturbines, and an Improved Type," ASME GT2003-38871.

TURBOMACHINERY

Benini, E., Toffolo, A. and Lazzaretto, A., 2003a, "Centrifugal Compressor of a 100 KW Microturbine: Part 1 - Experimental and Numerical Investigations on Overall Performance," ASME paper GT2003-38152.

Benini, E. and Toffolo, A., 2003b, "Centrifugal Compressor of a 100 KW Microturbine: Part 2 - Numerical Study of Impeller-Diffuser Interaction," ASME paper GT2003-38153.

Benini, E. and Toffolo, A., 2003c, "Centrifugal Compressor of a 100 KW Microturbine: Part 3 – Optimization of Diffuser Apparatus," ASME paper GT2003-38154.

Biba, Y. I., 2002, "The Impact of Volute Versus Collector on Centrifugal Compressor Performance," ASME GT-2002-30375.

Bonaiuti, D., Arnone, A., Hah, C. and Hayami, H., 2002, "Development of Secondary Flow Field in a Low Solidity Diffuser in a Transonic Centrifugal Compressor Stage," ASME paper GT-2002-30371.

Cui, M. M., 2002, "Effect of Suction Elbow and Inlet Guide Vanes on Flow Field in a Centrifugal Compressor Stage," ASME paper GT-2002-30376.

Ebaid, M. S. Y., Bhinder, F. S., Khdairi, G. H. and El-Hasan, T. S., 2002, "A Unified Approach for Designing a Radial Flow Gas Turbine," ASME paper GT-2002-30578.

Ferrara, G., Ferrari, L., Mengoni, C. P., Lucia, M. D. and Baldassarre, L., 2002a, "Experimental Investigation and Characterization of the Rotating Stall in a High Pressure Centrifugal Compressor: Part 1: Influence of Diffuser Geometry on Stall Inception," ASME paper GT-2002-30389.

Ferrara, G., Ferrari, L., Mengoni, C. P., Lucia, M. D. and Baldassarre, L., 2002b, "Experimental Investigation and Characterization of the Rotating Stall in a High Pressure Centrifugal Compressor: Part 2: Influence of Diffuser Geometry on Stage Performance," ASME paper GT-2002-30390.

Ibaraki, S., Matsuo, T., Kuma, H., Sumida, K. and Suita, T., 2002, "Aerodynamics of a Transonic Centrifugal Compressor Impeller," ASME paper GT-2002-30374.

Kang, S., Johnston, J. P., Arima, T., Matsunaga, M., Tsuru, H. and Prinz, F. B., 2003, "Micro-Scale Radial-Flow Compressor Impeller Made of Silicon Nitride –Manufacturing and Performance," ASME paper GT2003-38933.

Krain, H., 2003, "Review of Centrifugal Compressor's Application and Development," ASME paper GT2003-38971.

Mukkavilli, P., Raju, G. R., Dasgupta, A. and Murty, G. V. R., 2002, "Flow Studies on a Centrifugal Compressor Stage with Low Solidity Diffuser Vanes," ASME paper GT-2002-30386.

Oh, J., 2002a, "Investigation of Off-Design Performance of Vaned Diffusers in Centrifugal Compressors Part 1: A Channel-Wedge Diffuser," ASME paper GT-2002-30387.

Oh, J., 2002b, "Investigation of Off-Design Performance of Vaned Diffusers in Centrifugal Compressors Part 2: A Low-Solidity Cascade Diffuser," ASME paper GT-2002-30388.

Plafreyman, D. and Martinez-Botas, R. F., 2002, "Numerical Study of the Internal Flow Field Characteristics in Mixed Flow Turbines," ASME paper GT-2002-30372.

Rodgers, C., 2003, "The Characteristics of Radial Turbines for Small Gas Turbines," ASME paper GT2003-38026.

Schreiber, H., Steinert, W., Sonoda, T. and Arima, T., 2003, "Advanced High Turning Compressor Airfoils for Low Reynolds Number Condition: Part 2: Experimental and Numerical Analysis," ASME paper GT2003-38477.

Sonoda, T., Yamaguchi, Y., Arima, T., Olhofer, M., Sendhoff, B. and Schreiber, H., 2003, "Advanced High Turning Compressor Airfoils for Low Reynolds Number Condition: Part 1: Design and Optimization," ASME paper GT2003-38458.

Turunen-Saaresti, T., Reunanen, A. and Larjola, J., 2002, "The Time-Accurate Numerical Simulation of a Centrifugal Compressor," ASME paper GT-2002-30385.

Yaras, M. I. and Orsi, P., 2002, "Measurements of the Effects of Periodic Inflow Unsteadiness on the Aerodynamics of a Fishtail Diffuser," ASME paper GT-2002-30455.

Zangeneh, M., Vogt, D. and Roduner, C., 2002, "Improving a Vaned Diffuser for a Given Centrifugal Impeller by 3D Inverse Design," ASME paper GT-2002-30621.

STREAMLINE CURVATURE

Brereton, G. and Shih, T., 2001, "Turbulence Modeling in Simulation of Gas Turbine Flow and Heat Transfer," Heat Transfer in Gas Turbine Systems, Vol. 934, pp 52-63.

Kestoras, M. D. and Simon, T. W., 1997, "Turbulent Transport Measurements in a Heated Boundary Layer: Combined Effects of Free-Stream Turbulence and Removal of Concave Curvature," ASME J. Heat Transfer , Vol. 119, No. 3, pp. 413-419.

Ligrani, P. M. and Hedlund, C. R., 2003, "Experimental Surface Heat Transfer and Flow Structure in a Curved Channel With Laminar, Transitional, and Turbulent Flows," ASME paper GT2003-38734.

Schultz, M. P. and Volino, R. J., 2001, "Effects of Concave Curvature on Boundary Layer Transition Under High Free-Stream Turbulence Conditions," ASME paper 2001-GT-0191.

Schwarz, A. C., Plesniak, M. W. and Murthy, S. N. B., 2002, "Response of Turbulent Boundary Layers to Multiple Strain Rates," Journal of Fluid Mechanics, Vol. 458, pp. 333-377.

Smith, B. R., 2003, "An Explicit Algebraic Stress Model for Simulation of Flows with Streamwise Curvature," AIAA paper 2003-3738.

Volino, R. J., and Simon, T. W., 1994, "An Application of Octant Analysis to Turbulent and Transitional Flow Data," Journal of Turbomachinery, Vol. 116, No. 4, pp. 752-758.

Volino, R. J., and Simon, T. W., 1995, "Bypass Transition in Boundary Layers Including Curvature and Favorable Pressure Gradient Effects," ASME J. of Turbomachinery, Vol. 117, No. 1, pp. 166-174.

Volino, R. J., and Simon, T. W., 1997a, "Boundary Layer Transition under High Free-Stream Turbulence and Strong Acceleration Conditions: Part 1, Mean Flow Results," ASME J. of Heat Transfer, Vol. 119, No. 3, pp. 420-426.

Volino, R. J., and Simon, T. W., 1997b, "Boundary Layer Transition under High Free-Stream Turbulence and Strong Acceleration Conditions: Part 2, Turbulent Transport Results," ASME J. of Heat Transfer, Vol. 119, No. 3, pp. 427-432.

Volino, R. J., and Simon, T. W., 2000, "Spectral Measurements in Transitional Boundary Layers on a Concave Wall under High and Low Free-Stream Turbulence Conditions," J. of Turbomachinery, Vol. 122, pp. 450-457.

LOW REYNOLDS NUMBER EFFECTS AND BOUNDARY LAYER TRANSITION

Abu-Ghannam, B. J., and Shaw, R., 1980, "Natural Transition of Boundary Layers – The Effects of Turbulence, Pressure Gradient, and Flow History," Journal of Mechanical Engineering Science, Vol. 22, No. 5, pp. 213-228.

Boyle, R. J. and Simon, F. F., 1998, "Mach Number Effects of Turbine Blade Transition Length Prediction," ASME 98-GT-367.

Brunner, S., Fottner, L. and Schiffer, H.-P., 2000, "Comparison of Two Highly Loaded Low Pressure Turbine Cascades under the Influence of Wake-Induced Transition," ASME paper 2000-GT-268.

Byerley, A. R., Störmer, O., Baughn, J. W., Simon, T. W., Treuren, K. W. V. and Jörg List, J., 2002, "Using Gurney Flaps to Control Laminar Separation on Linear Cascade Blades," ASME paper GT-2002-30662.

Cardamone, P., Stadtmüller, P. and Fottner, L., 2002, "Numerical Investigation of the Wake-Boundary Layer Interaction on a Highly Loaded LP Turbine Cascade Blade," ASME paper GT-2002-30367.

Cebeci, T. and Smith, A. M. O., 1974, "Analysis of Turbulent Boundary Layers," Academic Press, New York.

Chakka, P. and Schobeiri, M. T., 1999, "Modeling Unsteady Boundary Layer Transition on a Curved Plate under Periodic Unsteady Flow Conditions: Aerodynamic and Heat Transfer Investigations," ASME Journal of Turbomachinery, vol. 121, Jan. 1999, pp. 88-97.

Chernobrovkin, A. and Lakshminarayana, B., 2000, "Unsteady Viscous Flow Causing Rotor-stator Interaction in Turbines, Part 2: Simulation, Integrated Flowfield, and Interpretation," Journal of Propulsion & Power. Vol. 16 No. 5, pp. 751-759.

Chong, T. P. and Zhong, S., 2003, "On the Three-Dimensional Structure of Turbulent Spots," ASME paper GT2003-38435.

Coton, T., Arts, T., Lefebvre, M. and Liamis, N., 2002, "Unsteady and Calming Effects Investigation on a Very High Lift LP Turbine Blade – Part I: Experimental Analysis," ASME paper GT-2002-30227.

Davis, R. L., Carter, J. E. and Reshotko, E., 1985, "Analysis of Transitional Separation Bubbles on Infinite Swept Wings," AIAA Paper # AIAA-85-1685.

Dhawan, S. and Narasimha, R. 1958, "Some Properties of Boundary Layer Flow During the Transition from Laminar to Turbulent Motion," J. Fluid Mech., Vol. 3, pp. 418-436.

D'Ovidio, A., Harkins, J. A. and Gostelow, J. P., 2001a, "Turbulent Spots in Strong Adverse Pressure Gradients Part 1 – Spot Behavior," ASME paper 2001-GT-0194.

D'Ovidio, A., Harkins, J. A. and Gostelow, J. P., 2001b, "Turbulent Spots in Strong Adverse Pressure Gradients Part 2 – Spot Propagation and spreading Rate," ASME paper 2001-GT-0406.

Drela, M., 1995, "MISES Implementation of Modified Abu-Ghannam/Shaw Transition Criterion," MIT Aero-Astro.

Emmons, H. W., 1951, "The Laminar-Turbulent Transition in a Boundary Layer—Part I," Journal of the Aeronautical Sciences, July, 1951, pp 490-498.

Eulitz, F. and Engel, K., 1998, "Numerical Investigation of Wake Interaction in a Low Pressure Turbine," ASME 98-GT-563.

Funazaki, K. and Aoyama, Y., 2000, "Studies on Turbulence Structure of Boundary Layers Disturbed by Moving Wakes," ASME paper 2000-GT-0272.

Funazaki, K., Yamada, K. and Kato, Y., 2003, "Studies on Effects of Periodic Wake Passing upon a Blade Leading Edge Separation Bubble: Experimental Investigation using a Simple Leading Edge Model," ASME paper GT2003-38281.

Gier, J., Ardey, S. and Heisler, A., 2000, "Analysis of Complex Three-Dimensional Flow in a Three-Stage LP Turbine by Means of Transitional Navier-Stokes Simulation," ASME paper 2000-GT-645.

Gombert, R. and Höhn, W., 2001, "Unsteady Aerodynamical Blade Row Interaction in a New Multistage Research Turbine – Part 1: Experimental Investigation," ASME paper 2001-GT-0306.

Gostelow, J. P., Blunden, A. R. and Walker, G. J., 1994, "Effects of Free-Stream Turbulence and Adverse Pressure Gradients on Boundary Layer Transition," Journal or Turbomachinery, July 1994, Vol. 116.

Gostelow, J. P. and Thomas, R. L., "Response of a Laminar Separation Bubble to an Impinging Wake," ASME GT2003-38972.

Hodson, H. P., Addison, J. S. and Shepherdson, C. A., 1992, "Models for Unsteady Wake-induced Transition in Axial Turbomachines," J. Phys. III 2 (1992) pp. 545-574.

Höhn, W., Gombert, R. and Kraus, A., 2001, "Unsteady Aerodynamical Blade Row Interaction in a New Multistage Research Turbine Part 2: Numerical Investigation," ASME paper 2001-GT-0307.

Höhn, W. and Heinig, K., 2000, "Numerical and Experimental Investigation of Unsteady Flow Interaction in Low Pressure Multistage Turbine," ASME paper 2000-GT-437.

Houtermans, R., Coton, T. and Arts, T., 2003, "Aerodynamic Performance of a very High Lift LP Turbine Blade with Emphasis on Separation Prediction," ASME paper GT2003-38802.

Howell, R. J., Hodson, H. P., Schulte, V., Heinz-Peter Schiffer, H., Haselbach, F. and Harvey, N. W., 2001, "Boundary Layer Development in the BR710 and BR715 LP Turbines -The Implementation of High Lift and Ultra High Lift Concepts," ASME paper 2001-GT-0441.

Hu, J. and Fransson, T. H., 2000, "Numerical Performance of Transition Models in Different Turbomachinery Flow Conditions: A comparative Study," ASME paper 2000-GT-520.

Jiang, N. and Simon, T. W., 2003a, "Modeling Laminar-to-Turbulent Transition in a Low-Pressure Turbine Flow which is Unsteady due to Passing Wakes: Part I, Transition Onset," ASME paper GT2003-38787.

Jiang, N. and Simon, T. W., 2003b, "Modeling Laminar-to-Turbulent Transition in a Low-Pressure Turbine Flow which is Unsteady due to Passing Wakes: Part I, Transition Path," ASME paper GT2003-38963.

Jiang, N. and Simon, T. W., 2003c, "The Influence of Unsteady Acceleration and Turbulence Intensity on Transition in low-Pressure Turbines," AIAA paper 2003-3630

Johnson, M. W., 2002, "Prediction Transition Without Empiricism or DNS," ASME paper GT-2002-30238.

Johnson, M. W., 2003, "A Receptivity Based Transition Model," ASME paper GT2003-38073.

Kaszeta, R. W., 2000, Experimental Investigation of Transition to Turbulence as Affected by Passing Wakes, Ph. D. Thesis, University of Minnesota, Department of Mechanical Engineering.

Kaszeta, R. W., and Simon, T. W., 2002, "Experimental Investigation of Transition to Turbulence as Affected by Passing Wakes," NASA/CR-2002-212104.

Kaszeta, R. W., Simon, T. W. and Ashpis, D., 2001, "Experimental Investigation of Transition to Turbulence as Affected by Passing Wakes," ASME paper 2001-GT-0195.

Kaszeta, R. W., Simon, T. W., Ottaviani, F. and Jiang, N., 2003, "The Influence of Wake Passing Frequency and Elevated Free Stream Turbulence Intensity on Transition in Low-Pressure Turbines," AIAA paper 2003-3633.

Kim, K. and Crawford, M. E., 1998, "Prediction of Unsteady Wake-passing Effects on Boundary Layer Development," ASME HTD-Vol. 361-3/PID-Vol. 3.

Kim, K. and Crawford, M. E., 2000, "Prediction of Transitional Heat Transfer Characteristics of Wake-affected Boundary Layers," ASME Journal of Turbomachinery, vol. 122, pp. 78-87.

Lakshminarayana, B., Chernobrovkin, A., and Ristic, D., 2000, "Unsteady Viscous Flow Causing Rotor-Stator Interaction in Turbines, Part 1: Data, Code Pressure," Journal of Propulsion and Power, Vol. 16, No. 5, 2000, pp. 744-750.

Liu, J. S., Celestina, M. L., Heitland, G. B., Bush, D. B., Mansour, M. L. and Adamczyk, J. J., 2002, "Low Pressure Turbine Lapse Rate Study: CFD Model vs. Rig Data," ASME paper GT-2002-30542.

Lodefier, K., Merci, B., De Langhe, C. and Dick, E., 2003, "Transition Modelling with the SST Turbulence Model and an Intermittency Transport Equation," ASME paper GT2003-38282.

Lou, W. and Hourmouziadis, J., 2000 "Separation Bubbles under Steady and Periodic-Unsteady Main Flow Conditions," ASME paper 2000-GT-0270.

Mayle, R. E., 1991, "The Role of Laminar-Turbulent Transition in Gas Turbine Engines," ASME J. Turbomachinery, 113, pp. 509-537.

Narasimha, R., 1957, "On the Distribution of Intermittency in the Transition Region of a Boundary Layer," Journal of the Aeronautical Sciences, Vol. 24, pp 711-712.

Narasimha, R., 1985, "The Laminar-Turbulent Transition Zone in the Boundary Layer," Prog. Aerospace Sci. Vol. 22, pp. 29-80,1985.

Nayeri, C. and Höhn, W., 2003, "Numerical Study of the Unsteady Blade Row Interaction in a Three-Stage Low Pressure Turbine," ASME paper GT2003-38822.

Palma, P. D., 2002, "Numerical Analysis of Turbomachinery Flows with Transitional Boundary Layers," ASME paper GT-2002-30223.

Qiu, S., 1996, "An Experimental Study of Laminar to Turbulent Flow Transition with Temporal and Spatial Acceleration Effects," Ph. D. Thesis, University of Minnesota, Department of Mechanical Engineering.

Qiu, S. and Simon, T. W., 1997, "An Experimental Investigation of Transition as Applied to Low Pressure Turbine Suction Surface Flows," ASME Paper 97-GT-455.

Radomsky, R. W. and Thole, K. A., 2001, "Detailed Boundary Layer Measurements on a Turbine Stator Vane at Elevated Freestream Turbulence Levels," ASME 2001-GT-0169.

Ramesh, O. N. and Hodson, H. P., 1999, "A New Intermittency Model Incorporating the Calming Effect," Third European Conference on Turbomachinery, 1999.

Roach, P. E. and Brierley, D. H., 2000, "Bypass Transition Modelling: A New Method which Accounts for Free-stream Turbulence Intensity and Length Scale," ASME 2000-GT-278.

Roberts, W. B., 1980, "Calculation of Laminar Separation Bubbles and their Effect on Airfoil Performance," AIAA Journal, Vol. 18, No. 1, pp. 25-31.

Roberts, S. K., and Yaras, M. I., 2003a, "Measurements and Prediction of Free-Stream Turbulence and Pressure-Gradient Effects on Attached-Flow Boundary-Layer Transition," ASME paper GT2003-38261.

Roberts, S. K., and Yaras, M. I., 2003b, "Effects of Periodic Unsteadiness, Free-Stream Turbulence and Flow Reynolds Number on Separation-Bubble Transition," ASME paper GT2003-38262.

Roux, J. M., Lefebvre, M. and Liamis, N., 2002, "Unsteady and Calming Effects Investigation on a Very High Lift LP Turbine Blade - Part II: Numerical Analysis," Proceedings of ASME paper GT-2002-30228.

Roux, J. M., Mahe, P., Sauthier, B. and Duboue, J. M., 2001, "Aerothermal Predictions with Transition Models for High-Pressure Turbine Blades," Proc. Instn. Mech. Engrs., Vol. 215, Part A, pp 735-742.

Sanz, W. and Platzer, M. F., 2002, "On the Numerical Difficulties in Calculating Laminar Separation Bubbles," ASME paper GT-2002-30235.

Schobeiri, M. T. and Chakka, P., 2002, "Prediction of Turbine Blade Heat Transfer and Aerodynamics Using a New Unsteady Boundary Layer Transition Model," International Journal of Heat and Mass Transfer, 45, 2002, pp. 815-829.

Schobeiri, M. T., Chakka, P. and Pappu, K., 1998, "Unsteady Wake Effects on Boundary Layer Transition and Heat Transfer Characteristics of a Turbine Blade," ASME paper 98-GT-291.

Schobeiri, M. T., Ozturk, B. and Ashpis, D. E., 2003, "On the Physics of Flow Separation along a Low Pressure Turbine Blade under Unsteady Flow Conditions," ASME paper GT2003-38917.

Schobeiri, M. T. and Pappu, K., 1997, "Experimental Study on the Effect of Unsteadiness on Boundary Layer Development on a Linear Turbine Cascade," Experiments in Fluids, Vol. 23, pp. 306-316.

Schubauer, G. B., and Klebanoff, P. S., 1955, "Contributions on the Mechanics of Boundary Layer Transition," NACA TN 3489 (1955) and NACA Rep. 1289(1956).

Schultz, M. P. and Volino, R. J., 2001, "Effects of Concave Curvature on Boundary Layer Transition under High Free-Stream Turbulence Conditions," ASME paper 2001-GT-0191.

Simon, T. W., Qiu, S. and Yuan, K., 2000, "Measurements in a Transitional Boundary Layer under Low-Pressure Turbine Airfoil Conditions," NASA-CR - 2000-209957.

Solomon, W. J., 2000, "Effects of Turbulence and Solidity on the Boundary Layer Development in a Low Pressure Turbine," ASME paper 2000-GT-0273.

Solomon, W. J., Walker, G. J. and Gostelow, J. P., 1996,

"Transition Length Prediction for Flows with Rapidly Changing Pressure Gradients," Transactions of the ASME J. of Turbomachinery, Vol. 118, pp. 744-751.

Spalart, P. R. and Allmaras, S. R., 1992, "A One-equation Turbulence Model for Aerodynamic Flows," AIAA 92-0439.

Stadtmuller, P., Fottner, L. and Fiala, A., 2000, "Experimental and Numerical Investigation of Wake-induced Transition on a Highly Loaded LP Turbine at Low Reynolds Numbers," ASME paper 2000-GT-0269.

Stieger, R. D. and Hodson, H. P., 2003, "The Transition Mechanism of Highly-Loaded LP Turbine Blades," ASME paper GT2003-38304.

Stieger, R. D., Hollis, D., and Hodson, H. P., 2003, "Unsteady Surface Pressures due to Wake Induced Transition in a Laminar Separation Bubble on a LP Turbine Cascade," ASME paper GT2003-38303.

Suzen, Y. B., Xiong, G. and Huang, P. G., 2000, "Predictions of Transitional Flows in a Low-Pressure Turbine using an Intermittency Transport Equation," AIAA paper A00-33926.

Suzen, Y. B. and Huang, P. G., 2003 "Numerical Simulation of Wake Passing on Turbine Cascades," AIAA paper 2003-1256.

Suzen, Y. B., Huang, P. G., Volino, R. J., Corke, T. C., Thomas, F. O., Huang, J., Lake, J. P. and King, P. I., 2003, "A Comprehensive CFD Study of Transitional Flows in Low-Pressure Turbines under a Wide Range of Operating Conditions," AIAA paper 2003-3591.

Teusch, R., Brunner, S., Fottner, L. and Swobada, M., 2000, "The Influence of Multimode Transition Initiated by Periodic Wakes on the Profile Loss of a Linear Compressor Cascade," ASME paper 2000-GT-271.

Thurso, J. and Stoffel, B., 2001, "Numerical Simulation of Wake Velocity and Wake Turbulence Effects on Unsteady Boundary Layer Transition," Proceedings of the Institution of Mechanical Engineers. Part A, Journal of Power & Energy. Vol. 215 No. 6 pp. 753-762.

Vicedo, J., Dawes, W. N., Vilmin, S. and Savill, A. M., 2003, "Intermittency Transport Modeling of Separated Flow Transition," ASME paper GT2003-38719.

Victor, X. S. and Houdeville, R., 2000, "Influence of Periodic Wakes on the Development of a Boundary Layer," Aerosp. Sci. Technol. Vol. 4, pp. 371-381.

Vilmin, S., Hodson, H. P., Savill, A. M. and Dawes, W. N., 2003, "Predicting Wake-Passing Transition in Turbomachinery using an Intermittency-Conditioned Modelling Approach," AIAA paper 2003-3995.

Volino, R. J., 2002a, "An Investigation of the Scales in Transitional Boundary Layers under High Free-Stream Turbulence Conditions," ASME Paper GT-2002-30233.

Volino, R. J., 2002b, "Separated Flow Transition under Simulated Low-Pressure Turbine Airfoil Conditions: Part 1 – Mean Flow and Turbulence Statistics," ASME GT-2002-30236.

Volino, R. J., 2002c, "Separated Flow Transition under Simulated Low-Pressure Turbine Airfoil Conditions: Part 2 – Turbulence Spectra," ASME paper GT-2002-30237.

Volino, R. J., 2003a, "Passive Flow Control on Low-Pressure Turbine Airfoils," ASME paper GT2003-38728.

Volino, R. J., 2003b, "Separation Control on Low-Pressure Turbine Airfoils Using Synthetic Vortex Generator Jets," ASME paper GT2003-38729.

Volino, R. J. and Hultgren, L. S., 2000, "Measurements in Separated and Transitional Boundary Layers under Low-Pressure Turbine Airfoil Conditions," ASME paper 2000-GT-0260.

Volino, R. J. and Murawski, C. G., 2003, "Separated Flow Transition in a Low Pressure Turbine Cascade – Mean Flow and Turbulence Spectra," ASME paper GT2003-38727.

Volino, R. J., Schultz, M. P. and Pratt, C. M., 2001, "Conditional Sampling in a Transitional Boundary Layer under High Free-Stream Turbulence Conditions," ASME 2001-GT-0192.

Walsh, E., Myose, R., and Davies, M., 2002, "A Prediction Method for the Local Entropy Generation Rate in a Transitional Boundary Layer with a Free Stream Pressure Gradient," ASME paper GT-2002-30231.

Walters, D. K. and Leylek, J. H., 2003a, "A CFD Study of Wake-Induced Transition on a Compressor-Like Flat Plate," ASME paper GT2003-38680.

Walters, D. K. and Leylek, J. H., 2003b, "Simulation of Transitional Boundary-Layer Development on a Highly-Loaded Turbine Cascade with Advance RANS Modeling," ASME paper GT2003-38664.

Wang, T. and Rice, M. C., 2003, "Effect of Elevated Free-Stream Turbulence on Transitional Heat Transfer over Dual-Scaled Rough Surfaces," ASME paper GT2003-38835.

Wolff, S., Brunner, S. and Fottner, L., 2000, "The Use of Hot-Wire Anemometry to Investigate Unsteady Wake-Induced Boundary-Layer Development on a High Lift LP Turbine Cascade," ASME paper 2000-GT-49

Wu, X. and Durbin, P. A., 2000, "Boundary Layer Transition Induced by Periodic Wakes," ASME Journal of Turbomachinery, vol. 122, July 2000, pp. 442-449.

Yaras, M. I., 2001, "Measurement of The Effects of Pressure-Gradient History on Separation-Bubble Transition," ASME paper 2001-GT-0193.

Yaras, M. I., 2002, "Measurements of the Effects of Freestream Turbulence on Separation-Bubble Transition," ASME paper GT-2002-30232.